


Finite Element Modelling for Failure Prevention of Coated Piston Compression Ring

Prakash Chandra Mishra, VSSUT Burla, India*

Pragyan Tiwari, KIIT University, India

Fuad Khoshnaw, De Montfort University, UK

 <https://orcid.org/0000-0002-4467-1944>

ABSTRACT

Finite element simulation using ANSYS software is used to analyze the effect of coating layers of different materials on piston compression ring. Similar material properties to that in the actual structural piston-compression-ring were considered on the simulated model. Three different coating materials, MgZrO₃, La₂Zr₂O₆, 3YSZ, and NiCrAl as bond coat materials of 1.6 mm thickness were chosen to investigate the deformation, von Mises stress-strain, temperature distribution, heat flux of the core and coating layers. The results showed that the total elastic deformation was maximum for coating type MgZrO₆, which was equal to 1.767 μm and was higher by 0.46 times than uncoated ring, while maximum von Mises stress was observed for coating type La₂Zr₂O₆, which was higher by 1.69 times than that of the uncoated ring. Moreover, the maximum elastic strain was for type MgZrO₆, which was equal to 0.003576, higher by 12.33 times comparing with the uncoated ring. Also, temperature rise and heat flux were maximum in the case of the uncoated ring.

KEYWORDS

Compression Ring, Heat Flux, Stress-Strain, Temperature, Thermal Barrier Coating

INTRODUCTION

The sealing of combustion gas in an internal combustion (IC) engine is an essential requirement to obtain high-performance. An ideal piston ring needs to be designed to perform simultaneous sealing and sliding action without significant failures like wear or blow-by. Improper sealing may lead to gas blow-by or excessive cylinder liner wear. It is important to improve the wear resistance of ring through the coating, which can prevent it from rapid decay. Before discussing the coating strength, it is essential to understand the function of piston rings. The piston rings were first introduced in the reciprocating engine by (Ramsbottom, 2009) who showed how the friction is reduced and gas blow-by is restricted due to its implementation. In practice, mainly three types of piston rings - which are widely used in automotive - are compression ring, scraper/wiper ring, and oil control ring.

The efficiency of IC engines is reduced due to frictional losses out of piston ring and cylinder liner co-action. According to (Buyukkaya and Cerit, 2007) investigation, about 33% of the total heat is transferred to the cylinder wall via piston and then via piston ring. Therefore, to reduce friction loss and thermal fatigue - as a mode of failure—efficient engine cooling and better fuel economy

DOI: 10.4018/IJMMME.299057

*Corresponding Author

This article published as an Open Access article distributed under the terms of the Creative Commons Attribution License (<http://creativecommons.org/licenses/by/4.0/>) which permits unrestricted use, distribution, and production in any medium, provided the author of the original work and original publication source are properly credited.

are required. The main function of the rings is to seal the combustion chamber to minimize loss of power. This is achieved through proper lubrication and faster heat transfer through piston ring and cylinder wall. Generally, three or, minimum, two rings are necessary on most piston-cylinder systems. Usually, rings need to be loosely fitted to allow the expansion at elevated temperatures. However thermal deformation, with low clearance, may lead to welding - due to high friction - of rings with cylinder causing serious damage. On the other hand, if high clearance is provided then blow-by will occur thereby reducing the efficiency (Cerit,2011).

Generally, rings mostly are made of cast iron and usually coated with chromium and molybdenum to enhance the resistance against thermal deformation. The main problem with the piston ring as mentioned earlier is wear, due to which engine is required to be disassembled after standard 100,000 miles run of a vehicle for ring replacement. Such disassemble activities affect and lead to misalignment of the other engine components and reduce engine life. Therefore, to increase the lifetime of engine, different types of coating materials, which have high wear resistance, have been applied on rings and the results showed improvement of the ring durability and thereby reducing frequent engine maintenance.

To examine the reliability and level of improvement in which the coating process will add to engine performance, researchers relied for a long time on the experimentally obtained results. However, in the last decade, developing new numerical methods and simulations on coating strength have widely been applied by researchers to examine the performance of the coated materials. Finite element analysis (FEA) is effectively used in the design analysis of structural and mechanical elements. It has been used to analyze modes of failure, the effect of coating and up-gradation of existing designs, identifying ideal coating materials that provide the highest life and performance.

Buyukkaya and (Buyukkaya and Cerit,2007) used the 3D ANSYS method to analyze the thermal behavior of ceramic coating on four types of rings. The results showed that Al-Si and steel coated rings provide an increase of 48% and 35% in thermal conductivity respectively. Moreover, a partially coated piston ring with a ceramic coat improved the thermomechanical properties. (Cerit,2011) found that a bond coat thickness of 1.0 mm of NiCrAl, reduces the normal stress and increases the shear stress. While a 4.0 mm coat thickness of the same type of material helps to elevate the surface temperature to the order of 82°C (Sliwa et al, 2016) used FEA to simulate the stress distribution of components through PVD/CVD coating. They used Multilayer coatings of Ti/Ti (C, N)/CrN, Ti/Ti (C, N)/(Ti, Al) N, Ti/ (Ti, Si) N/ (Ti, Si) N, and Ti/DLC/DLC on surface of magnesium alloy. The simulated ANSYS results and experimentally determined x-ray diffraction pattern showed high similarities in this investigation.

(Bouzakis et al.,1998) investigated fatigue behavior using both ANSYS and experimental tests of PVD coatings on high-speed steel (HSS) cutting tool during milling a substrate. The results were compared and found compatible with both ANSYS and experimental work were done using a scanning electron microscope (SEM) and energy dispersive X-ray (EDX) analysis. (Holmberg et al, 2006) worked on a tribological model of 3D FEA stress simulation to analyze fracture conditions of surface coatings. They used scratch tester contact of the diamond spherical tip with a 200µm radius and sliding with increase load on 2µm thick titanium nitride coated steel surface to scratch the specimen.

(Funke et al.,1997) carried out combined characterization and FEM stress redistribution analysis during thermal cycling - of ZrO_2 , 7wt% Y_2O_3 of thermal barrier coating (TBC) with different porosity. The development of creep, at 1100°C and 500 hr, of thermal cycling, was started due to heating and subsequent cooling in zirconia, which was responsible for the debonding of the coated surface. Jiang- (Jiang-Hao *et al.*, 2013) developed a FEM model to estimate the elastic modulus of TBC. The numerical method was built based on image analysis, compared with binary gray image analysis of SEM. Moreover, the elastic modulus computed through 3D imaging was compared with that obtained from 2D computation performed on the cross-section. The computed results were 54% compatible with the experimental value.

(Dahm and Dearnly,2002) preferred plasma-based sputtering over graded coating for a piston ring, and this was attributed to better fatigue resistance to cyclic loading. (Davis et al., 2018) worked

on the in-situ application, e.g., piston ring, and found that Cr_2AlC in Ni-Mo-Al alloying significantly improves the mechanical properties. Such alloying shows good tribological properties such as adhesion, hardness, wear-resistance, and exfoliation. (Lima et al.,2013) used a numerical analysis method to study the effect of film thickness and coating material properties on the stress state of the nanocomposite. The results show that nanocomposite lowers the friction when applied in the piston compression ring.

(Lin et al.,2016) estimated the friction performance of TiSiCN nanocomposite used as a coating in the piston ring. The results showed that using the coating led to a 25% to 34% reduction in friction and 28% to 40% lower ring weight loss. (Sachit et al.,2018) showed that the hybrid nanocomposite, such as coating using powder metallurgy, gives better reinforcement of metal matrix composite. The performance of MoN as a coating material for diesel engine piston is observed by (Hazar,2010). Besides, (Cho and Lee,2009) reported that scuffing life is affected due to ring-liner friction. Other researchers (Mishra, 2013-a;2013-b; Henley,2009 and Mishra et al., 2015) recently, have worked on TBC which is commonly used in manufacturing automotive pistons, their results showed that, besides the reduction in the wear rate, TBC improves the adiabatic condition, such that the heat rejection rate decreases to improve thermal efficiency. (Hamid et al.,2020) developed a numerical model of fluid flow in CI engine to study turbulent flow, swirl, tumble, and cross tumble. (Lyu et al.,2020) studied the numerical method for friction reduction and wear resistance of cam-tappet pair considering both asperity and fluid friction mechanism.

The literature review mentioned above summarized that many researchers used simulation analysis to enhance the consistency of the theoretical results on the coating material. They were preferring to apply experimental works too to correlated both methods (Theoretical simulation and experimental observation). The coating materials like Al-Si, Ti, CrN, DLC, ZrO_2 , Y_2O_3 , Cr_2AlC , and TiSiCN were investigated in different applications including that of piston ring. But a comparative study is absent in the literature considering different options. In the current study, three different coating materials, MgZrO_3 , $\text{La}_2\text{Zr}_2\text{O}_6$, 3YSZ, and NiCrAl as bond coat materials will be considered as different cases and analysis will be carried out to understand the superior coating material among them for piston ring application. It will be under taken by computer simulation using ANSYS.

MATERIALS AND METHODS

The finite element analysis for the coating strength of the piston ring was carried out in this study using three different thermal barrier coating materials. Input parameters were found different for different coatings due to distinguished properties of coating materials. Temperature, total heat flux, elastic deformation, von misses stress and strain are different from case to case. Such analysis encourages further extending the work for fatigue and creep analysis of the in-situ piston ring.

Materials for the Model

Different coating material gives different coating strength in different environment of the application. Hence, it is desirable to study the structural strength of such coatings in the context of piston compression ring application. In this study, three different groups of samples were analyzed: low alloy steel with a composition of 0.8%C, 1.2% Al, 0.2% Mn, and 3.5% Si, as an uncoated ring, NiCrAl alloy as a bond coat ring, and coated rings (applying three different materials as coating layers which were MgZrO_3 , $\text{La}_2\text{Zr}_2\text{O}_6$, and 3YSZ). The bond coat of NiCrAl, maximum thickness 0.1mm, was applied in the core material of steel to achieve structural integrity and desired thermal properties for the piston compression ring. Variable wear resistance and thermal stability were investigated. The details of core ring material, bond coat, and three coating materials are given in Table 1.

Table 1. Properties of coating material

| Materials Properties | Steel Alloy | NiCrAl | MgZrO ₃ | La ₂ Zr ₂ O ₆ | 3YSZ |
|--|-------------|--------|--------------------|--|------|
| Density (Kg/m ³) | 7800 | 7870 | 5600 | 5740 | 6080 |
| Thermal conductivity (W/m K) | 25.3 | 16.1 | 0.8 | 1.56 | 2.12 |
| Coefficient of thermal expansion (10 ⁻⁶ K ⁻¹) | 12.5 | 12 | 0.8 | 9.1 | 10.7 |
| Young's modulus (GPa) | 210 | 90 | 46 | 175 | 200 |
| Poisson's ratio | 0.30 | 0.27 | 0.2 | 0.2 | 0.22 |

Fig. 1a shows the geometry of the ring, which is an incomplete circular ring– as suggested by (Mishra,2013-b) made of highly elastic material, shown in Table 1, has a parabolic profile with single point minima at outer face. Fig. 1b shows the inner face of a bevel shape that helps in allowing ring to flex during direction change.

Figure 1. Ring geometry, a: Ring pictorial sketch, b: Ring cross-sectional view

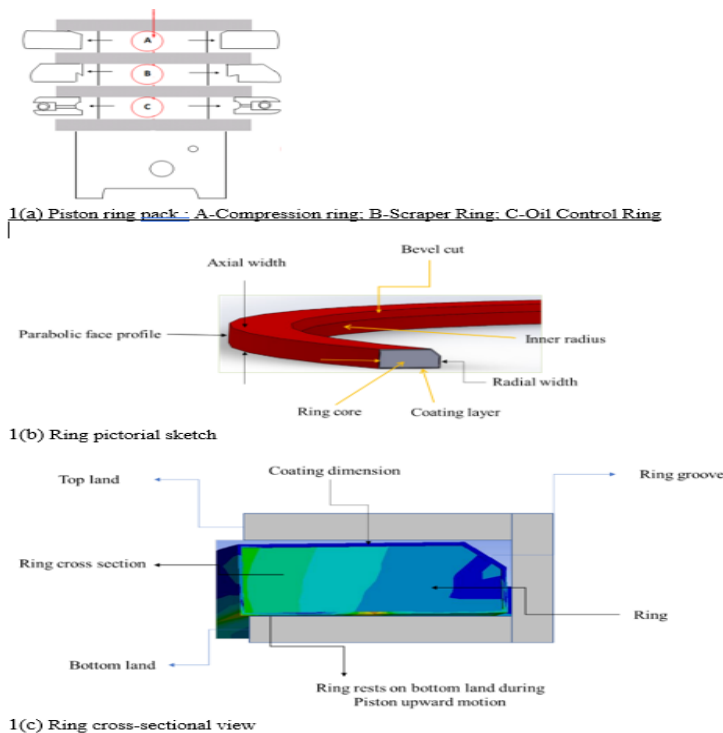


Table 2 shows the different ring dimensions. The ring with a bond coat and coating is considered as a single elastic element with layered elastic properties. The whole system of element processed appreciable thermal conductivities. Creep, corrosion, fatigue, and thermal degradations like redundant effects are neglected in this analysis. The ring is supposed to have a10 mm free end gap, while out of

the assembly - once mounted in the piston and fitted in the engine - the gap is squeezed to less than 0.3mm. This gap makes the blow-by negligible (Mishra,2013-b).

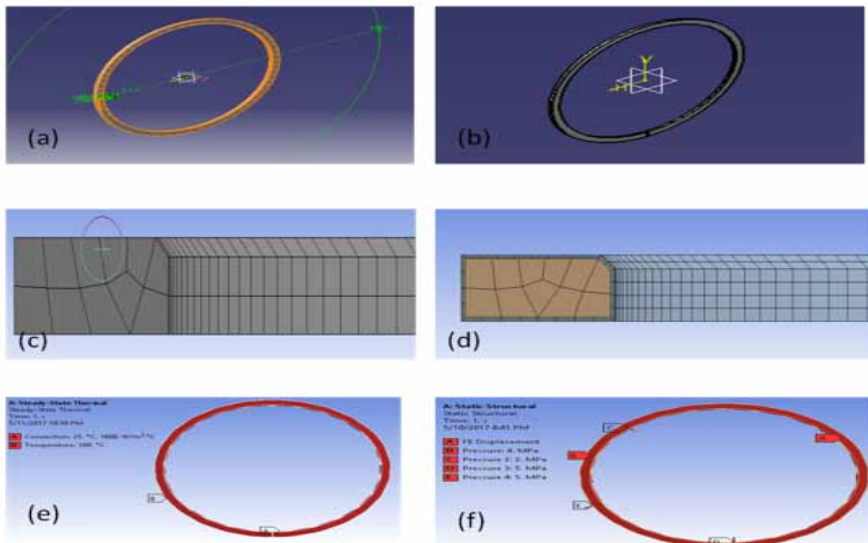
Table 2. Ring geometry details

| Nominal Diameter (d1) | 85 mm |
|-----------------------------------|--------|
| Ring Width (without coating) (h1) | 1.5 mm |
| Radial Width (a1) | 3.6 mm |
| Closed Gap (s1) | 0.3 mm |
| Coating | 0.1 mm |

Structural FEA Model

Fig.2 a-b shows the construction steps of the piston compression ring, which is an incomplete circular ring with a parabolic front profile and beveled back face. The next required step was to mesh the ring, which means generating a grid surface consisting of a number of points, called 'nodes', which can be carried out through a variety of options using the software. Fig. 2c and 2d show the mesh models of uncoated and coated rings respectively. The outcomes are calculated by solving the governing equations numerically at each node of the mesh.

Figure 2. Ring model, mesh and thermostatic boundary conditions, a: Ring model using shaft tools, b: Solid final model, c: Uncoated ring mesh view, d: Two-layer coated ring meshing, e: Thermal boundary conditions, f: Static boundary conditions



Discretizing the domain, ring geometry, for finite element mesh is a necessary step, as considering fine discretized mesh and choosing higher-order elements, will increase the data accuracy. This would be achieved through a grid-independent test, which means selecting a proper mesh by balancing the

accuracy of the solution and computational efficiency - called a mesh convergence study. Table 3 shows the meshing details for uncoated and two-layer coated rings. The number of nodes and elements are automatically fixed by ANSYS workbench, giving optimum results, based on machine capacity. Table 4 shows the mesh convergence of the model, based on that the number of elements/ nodes were fixed manually, by keeping the most accurate solution.

Table 3. Meshing details of uncoated and two-layer coating rings.

| Type of Model | No. of Nodes | No. of Elements |
|--------------------|--------------|-----------------|
| Zero-layer coating | 18607 | 3047 |
| Two-layer coating | 119695 | 17451 |

Table 4 also showed the effect of the element size on the number of nodes and elements. Because of grid variation, the corresponding changes in computed output parameters were monitored. A high number of elements cause the ring to shape finer and accurate. Further, the gas load and lubrication forces on the ring are pressure type, i.e. distributed load, whereas the reactions are point load type. The ring is assumed to rest on top land on the downward motion of the piston assembly, while in an upward motion, it rests on the bottom surface. Fig. 2e and 2f show the thermal boundary details and structural loading.

Table 4. Mesh convergence of the models

| Sl. No | Element Size (mm) | No. of Elements | Total Heat Flux (W/mm ²) | Directional Heat Flux (W/mm ²) | Total deformation (μm) | Equivalent stress (MPa) | Equivalent strain |
|--------|-------------------|-----------------|--------------------------------------|--|------------------------|-------------------------|-------------------|
| 1 | 0.8 | 175785 | 1.7969 | 1.3639 | 1.8235 | 99.52 | 0.0044554 |
| 2 | 0.9 | 140465 | 1.8494 | 1.3662 | 1.8077 | 99.197 | 0.0044381 |
| 3 | 1.0 | 119695 | 1.9088 | 1.3707 | 0.0017735 | 79.828 | 0.0035792 |
| 4 | 1.1 | 108920 | 1.9087 | 1.3706 | 1.7677 | 79.639 | 0.0035737 |
| 5 | 1.2 | 89957 | 1.8977 | 1.3777 | 0.6995 | 30.712 | 0.0013767 |

FEA Simulation

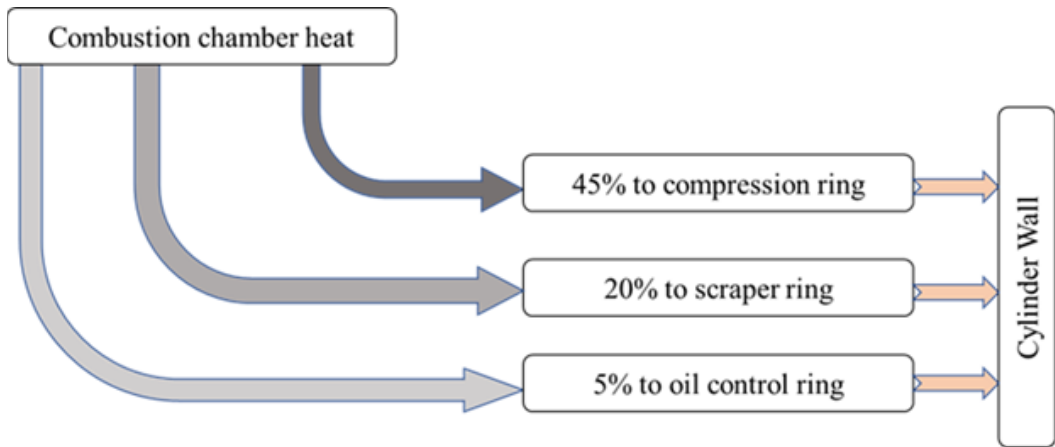
Pre-processing is the first step for FEM of the ring, in which the finite element mesh was created, then, the material properties of the coat and the substrate, load, and boundary conditions were defined. The pre-processing for the current analysis was carried out using ANSYS workbench, as the FEA tool for structural analysis, including nonlinear, linear, and dynamic studies. It also includes thermal analysis coupled with physics involving acoustics, thermo-structural, piezoelectric, and thermo-electric analysis. The next step is, analyzing the solution for the ring strength. It deals with the initiation of the governing equation from the model and solves it for stress-strain and deformation. For high strain rate cases, instead of implicit code, explicit codes are written and solved for better accuracy. Then, post-processing, which is the output is obtained as deformed wrong shape, profiles, and plots. Its validity with experimental results can be checked.

THERMAL FEA MODEL OF PISTON RINGS

The heat transfer model of the piston ring involves heat dissipation from the combustion chamber to the cylinder. As the heat is better known as energy in transit, flow due to temperature gradient happens mostly in three different modes: conduction, convection, and radiation. Heat transfer takes place in a combination of two or three modes in any of the real engineering applications.

There are several phenomena inside an IC engine, which are responsible for heat generation. The first and foremost is fuel combustion. Besides, contact and motion of piston subsystem components generate frictional heat. The heat transfer between a piston ring and cylinder liner is both by conduction and convection. The small clearance between ring and liner allows limited passage of lubricant film. Hence the convective heat transfer is not comparable to that due to conduction therefore ignored. This assumption reduces the number of variables needed for determining the energy flow for a general expression of heat conduction. Fig. 3 shows the heat transfer mode in the IC engine.

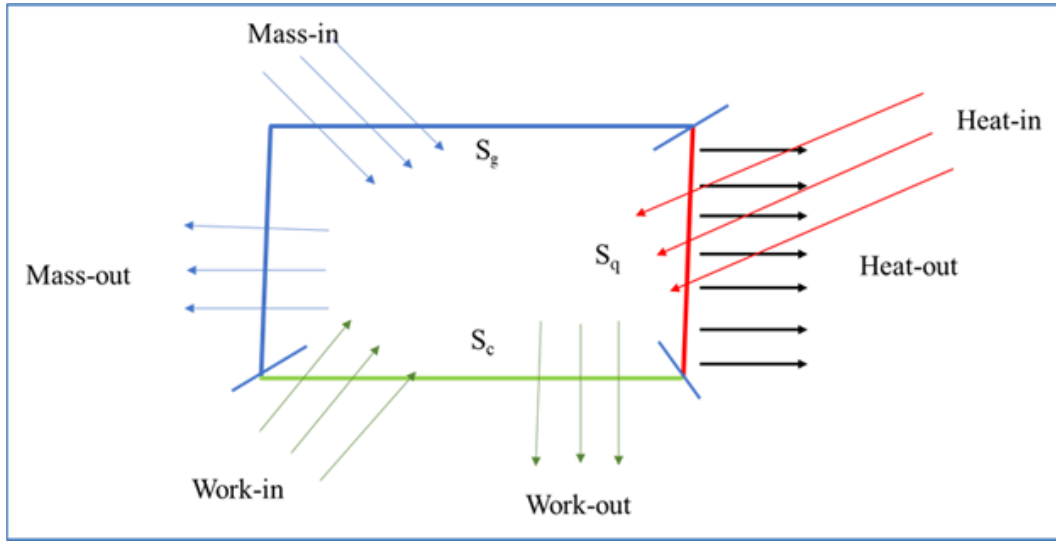
Figure 3. Probable heat transfer path in piston subsystem [22]



The formulation of heat transfer is shown in equation (1).

$$\left\{ \begin{array}{l} \text{div}(D\nabla T) + Q = 0 \\ q^n n = q'' \\ T = g \\ q'' = h(T - T_{amb}) \end{array} \right. \quad (1)$$

Figure 4. Control volume



where,

D: constitutive matrix

T: temperature gradient

Q: external heat supply

q_n : heat flux per unit area

n: normal vector

T: temperature

h: convective heat transfer coefficient

T_{amb} : ambient temperature

S_q , S_g and S_c are the boundaries of the body.

By multiplication with a test function, v and integration over the volume, given in the equation (2).

$$\int_v (\nabla v)^T D \nabla T dv = - \int_{S_q} v h ds - \int_{S_g} v q_n ds + \int_v v Q dv \quad (2)$$

Here, each node has one degree of freedom. Considering temperature in the node as a scalar quantity, the heat transfer model is discretized to create a finite number of elements. Fig. 4 shows the control volume and the physical boundary of the thermodynamic system.

RESULTS AND DISCUSSION

Static Structural Models

Fig. 5 shows the total deformation profile of the ring surface. Fig. 5a shows the maximum deformation of an uncoated ring, which is $1.2\mu\text{m}$, which is recorded on the mid of the ring axial width on the bottom of the ring. It is due to piston upward motion during compression and exhaust stroke. Subsequently, as shown in Fig. 5b, 5c and 5d, the deformation patterns were modified use of MgZrO_6 ($1.76\mu\text{m}$), $\text{La}_2\text{Zr}_2\text{O}_6$ ($1.22\mu\text{m}$), and 3YSZ ($1.19\mu\text{m}$) coatings respectively. It is due to variable elastic properties

of layered solids that distribute stress subsequent deformation. In these four types, the minimum deformation distribution occurs in the centroidal regions, in the present core ring alloy.

Figure 5. Ring FEM model for total deformation for uncoated and various coated rings

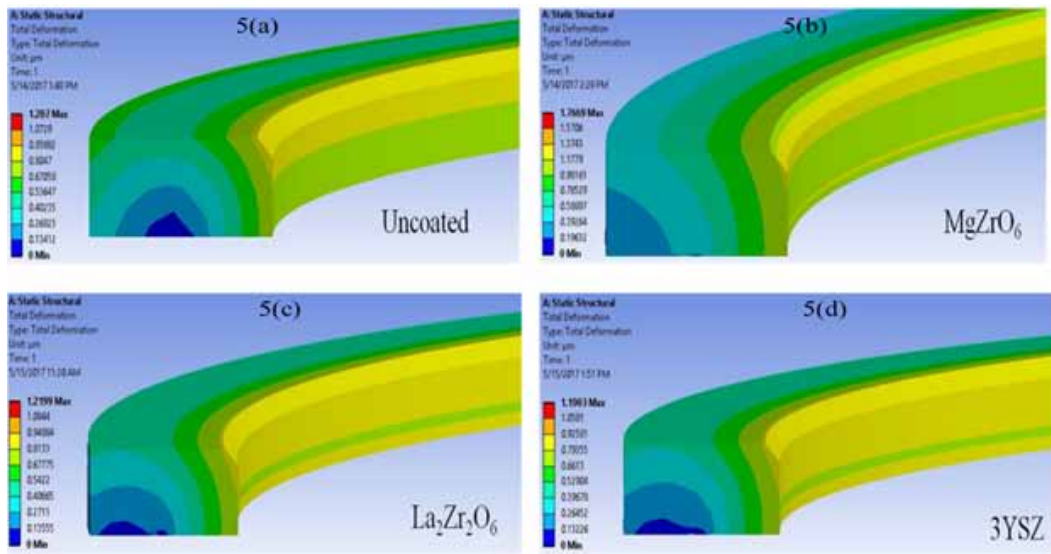


Figure 6. Ring FEM model for equivalent stress for uncoated and various coated rings

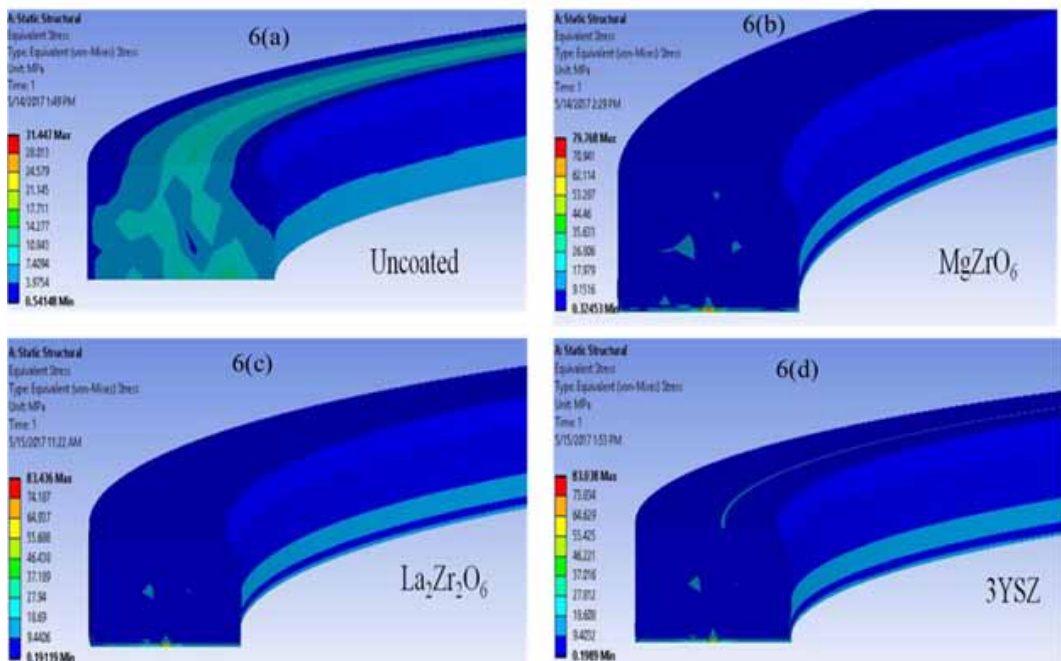
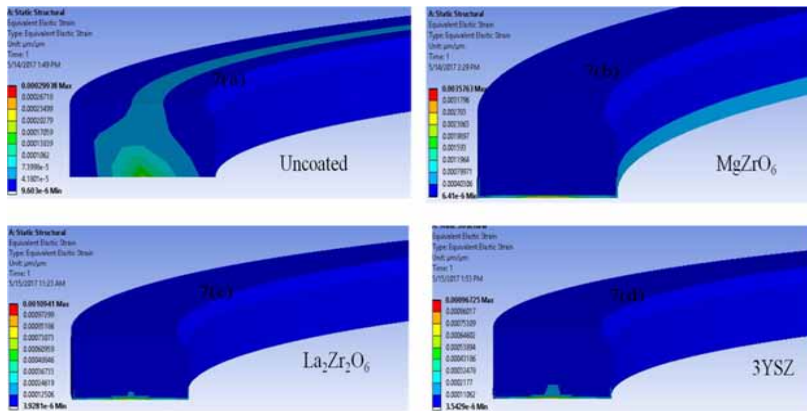


Fig. 6 a-d shows that $\text{La}_2\text{Zr}_2\text{O}_6$ develops maximum stress of 83.436 MPa, while other coatings such as MgZrO_6 and 3YSZ develop maximum stresses of 83.038 MPa and 79.768 MPa. This showed that the coated types increase the strength compared to the uncoated ring by 1.6 times. Fig. 7a shows the strain profile of the uncoated ring with a maximum strain value 299.3×10^{-6} . Figures 7b, 7c and 7d present corresponding maximum strain value of 356×10^{-6} , 109.4×10^{-6} , and 96.72×10^{-6} respectively. For a bond coat thickness of 1.6 mm as reported by (Cerit,2011), von Misses stress of 80 MPa developed at a radial distance of 30 to 36 mm of the ring, which is similar to this analysis.

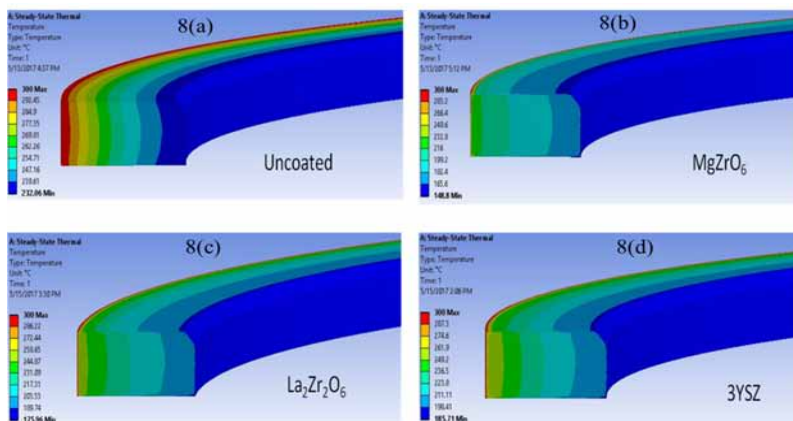
Figure 7. Ring FEM model for equivalent elastic strain for uncoated and various coated rings



Thermal FEA Results

Fig. 8a-d showed the temperature profile of uncoated piston ring, higher order of temperature penetration to a radial depth of ring in the top, face direction. The ring temperature matches with the results reported by (Buyukkaya and Cerit,2007). The reason can be attributed to the fact that the top location near to the combustion chamber and the face is subjected to severe repetitive sliding. Temperature difference ($T_{\max} - T_{\min} = \Delta\theta$) in this case is observed to be 68°C .

Figure 8. Ring FEM model for temperature profile of an uncoated and various coated rings



(Cerit,2011) estimated at the partially coated ring maximum temperature rise are 261.8°C and 311.1°C for coating thicknesses 0.3 mm and 0.5 mm, respectively. Due to three different coatings, the temperature difference was modified to 150°C, 125°C, and 115°C respectively for MgZrO₆, La₂Zr₂O₆ and 3YSZ coated rings respectively. Fig. 9a-d shows the heat flux of uncoated, MgZrO₆, La₂Zr₂O₆, and 3YSZ coated cases respectively. The heat flux for uncoated ranges, 3.4-23.73 W/m², while for coatings, were equal 8.7-15 W/m², 1.04-18.6 W/m² and 1.12-19 W/m² respectively.

Figure 9. Ring FEM model for total heat flux for uncoated and various coated rings

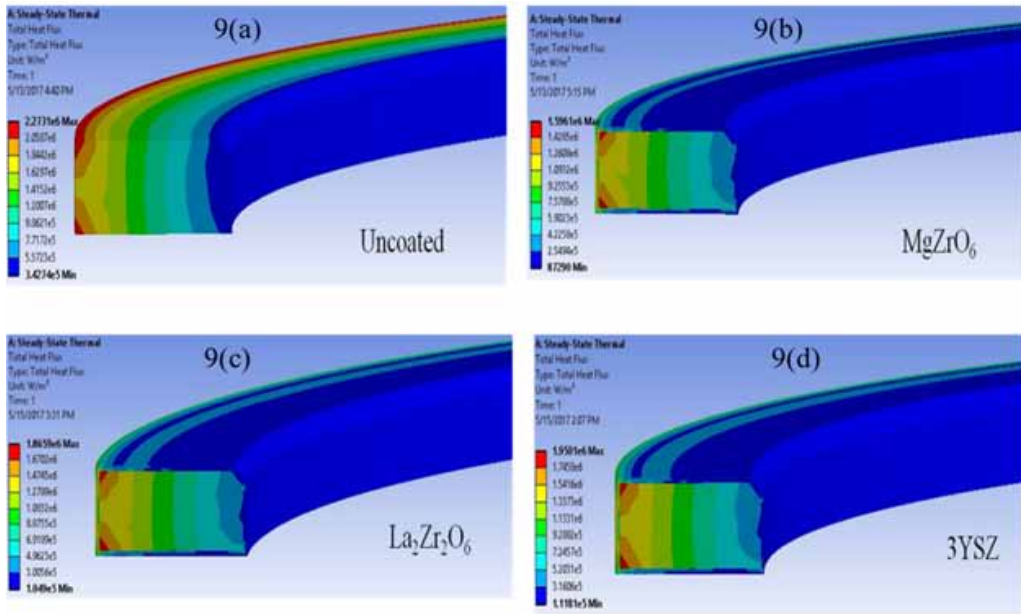


Table 5 shows the summary of the results related to the maximum value of all parameters such as total deformation, von Misses stress, equivalent strain, temperature, and heat flux. The maximum deformation occurs in the case of the MgZrO₆ coated ring, while the minimum is for 3YSZ. Furthermore, the uncoated ring developed the least stress compared to the coated rings. The highlighted values are maximum among the four considered cases. The coating enhanced the strength to 1.26 times that of uncoated one. The temperature is maximum in the case of the uncoated rings so also the heat flux, which suggests more heat transfer in case uncoated compared to coated rings.

Table 5. Summary of the Results

| Parameters Coatings | Temperature (°C) | Heat flux (W/m ²) in 10 ⁶ | Total deformation (μm) | Equivalent von-Misses stress (MPa) | Equivalent elastic strain (μm/μm) |
|--|------------------|--|------------------------|------------------------------------|-----------------------------------|
| Uncoated | 292 | 2.273 | 1.207 | 31.45 | 299 |
| MgZrO ₆ | 283 | 1.596 | 1.767 | 79.77 | 357 |
| La ₂ Zr ₂ O ₆ | 256 | 1.866 | 1.22 | 83.43 | 972 |
| 3YSZ | 287 | 1.95 | 1.19 | 83 | 860 |

Figure 10. temperature and heat flux correlation chart for different coating materials

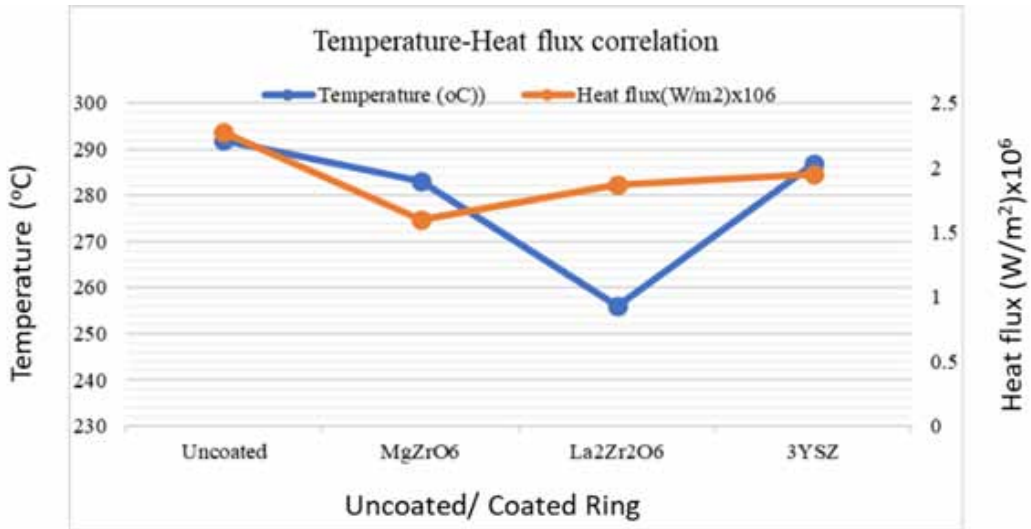


Fig.10 shows the combined graph for temperature and heat flux. The highest value of both parameters occurs in the case of an uncoated ring. The thermal conductivity is more in the case of an uncoated ring, while the 3YSZ coated ring has appreciable thermal conductivity. The order of thermal conductivity is in the order $3\text{YSZ} > \text{La}_2\text{Zr}_2\text{O}_6 > \text{MgZrO}_6$.

CONCLUSIONS

- The total elastic deformation is maximum for coating type MgZrO₆, of 1.767μm, and was higher by 1.46 times than the uncoated ring and more prone to failure.
- Maximum Von Misses stress of failure was observed for coating type La₂Zr₂O₆, higher by 2.694 times that of the uncoated ring.
- The maximum elastic strain of failure was for type MgZrO₆, which was equal to 0.3576%, higher by 12.33 times to the uncoated ring.
- The minimum temperature rise of 148°C was observed for type MgZrO₆ and was 1.057times more than that of the uncoated ring, whereas, in other types, it was higher and undesirable.
- Maximum heat flux, 2.27 W/m² was observed for the uncoated ring and was a minimum for the coating type MgZrO₆, was 1.375 times the uncoated ring.

COMPETING INTEREST

There is no compete interest

FUNDING

All India Council for Technical Education and Training (AICTE), New Delhi funded this research. Publisher has waived all fees.

AUTHORS' CONTRIBUTION

PT carried out the simulation of the research and carried out primary modeling and write up, **PCM** conceived the paper and carried out analysis, data curation and writing, **FK** carried out the result analysis and writing.

ACKNOWLEDGMENT

We are very much thankful to the All India Council for Technical Education and Training (AICTE), New Delhi for funding this research. The funding of AICTE through RPS grant-in-aid to carry out our research project entitled “Advanced Engine Technology for Sustainable Development of Automotive Industry” is here acknowledged, as was part of a collaboration with the School of Engineering and Sustainable Development, De Montfort University, Leicester in the United Kingdom.

REFERENCES

- Bouzakis, D., Efstathiou, K., Vidakis, N., Kallinkidis, D., Angos, S., Leyendecker, T., Erkensb, G., Fuss, H. G., & Wenke, R. (1998). Experimental and FEM Analysis of the Fatigue Behaviour of PVD Coatings on HSS Substrate in Milling. *CIRP Annals*, 47(1), 69–72. doi:10.1016/S0007-8506(07)62787-5
- Buyukkaya & Cerit. (2007). Thermal analysis of a ceramic coating diesel engine piston using 3-D finite element method. *Surface and Coatings Technology*, 202(2), 398–402. 10.1016/j.surfcoat.2007.06.006
- Cerit, M. (2011). Thermomechanical analysis of a partially ceramic coated piston used in an SI engine. *Surface and Coatings Technology*, 205(11), 3499–3505. doi:10.1016/j.surfcoat.2010.12.019
- Cho, D. H., & Lee, Y. Z. (2009). Evaluation of ring surfaces with several coatings for friction, wear and scuffing life. *Transactions of Nonferrous Metals Society of China*, 19(4), 992–996. doi:10.1016/S1003-6326(08)60393-3
- Dahm, K. L., & Dearnley, P. A. (2002). Novel plasma-based coatings for piston rings. *Tribology Series*, 40, 243–246. doi:10.1016/S0167-8922(02)80027-X
- Davis, D., Srivastava, M., Malathi, M., Panigrahi, B. B., & Singh, S. (2018). Effect of Cr₂AlC MAX phase addition on strengthening of Ni-Mo-Al alloy coating on piston ring: Tribological and twist-fatigue life assessment. *Applied Surface Science*, 449, 295–303. doi:10.1016/j.apsusc.2018.01.146
- Funke, C., Mailand, J. C., Siebert, B., Vaßen, R., & Stöver, D. (1997). Characterization of ZrO₂-7 wt.% Y₂O₃ thermal barrier coatings with different porosities and FEM analysis of stress redistribution during thermal cycling of TBCs. *Surface and Coatings Technology*, 94-95, 106–111. doi:10.1016/S0257-8972(97)00486-6
- Hamid, Idroas, Sa'ad, Heng, Sharzali, Mat, Alauddin, Shamsuddin, Shuib, & Abdullah. (2020). Numerical Investigation of Fluid Flow and In-Cylinder Air Flow Characteristics for Higher Viscosity Fuel Applications. *Processes MDPI*, 8, 439. 10.3390/pr8040439
- Hazar, H. (2010). Characterization of MoN coatings for pistons in a diesel engine. *Materials & Design*, 31(1), 624–627. doi:10.1016/j.matdes.2009.06.006
- Henley's Encyclopedia of Practical Engineering*. (1908). New York: The Normal W. Henley Publishing Company. <https://www.aaa.com/autorepair/articles/how-efficient-is-your-cars-engine>
- Holmberg, K., Laukkanen, A., Ronkainen, H., & Wallin, K. (2006). Tribological analysis of fracture conditions in thin surface coatings by 3D FEM modeling and stress simulations. *Tribology International*, 38(11-12), 1035–1049. doi:10.1016/j.triboint.2005.07.028
- Lima, L. G., Nunes, L. C., Souza, R. M., Fukumasu, N. K., & Ferrarese, A. (2013). Numerical analysis of the influence of film thickness and properties on the stress state of thin film-coated piston rings under contact loads. *Surface and Coatings Technology*, 215(25), 327–333. doi:10.1016/j.surfcoat.2012.04.102
- Lin, J., Wei, R., Bitsis, D. C., & Lee, P. M. (2016). Development and evaluation of low friction TiSiCNnano composite coatings for piston ring applications. *Surface and Coatings Technology*, 298, 121–131. doi:10.1016/j.surfcoat.2016.04.061
- Lyu, B., Meng, X., Zhang, R., & Cui, Y. (2020). A Comprehensive Numerical Study on Friction Reduction and Wear Resistance by Surface Coating on Cam/Tappet Pairs under Different Conditions. *Coatings*, 10(5), 485. doi:10.3390/coatings10050485
- Mishra, Prakhardeep, Bhattacharya, & Pandey. (2015). Finite element analysis for coating strength of piston compression in contact with cylinder liner: A Tribodynamic analysis. *Tribology in Industry*, 37(1), 42-54. <http://www.tribology.rs/journals/2015/2015-1/6.pdf>
- Mishra, P. C. (2013). Tribodynamic modeling of piston compression ring cylinder liner contact at high-pressure zone of engine cycle. *International Journal of Advanced Manufacturing Technology*, 66(5-8), 1075–1085. doi:10.1007/s00170-012-4390-y
- Mishra, P. C. (2013). Modeling for friction of four-stroke four-cylinder petrol engine. *Tribology in Industry*, 35(3), 237-245. <http://www.tribology.rs/journals/2013/2013-3/9.pdf>

Qiao, J.-H., Bolot, R., & Liao, H. (2013). Finite element modeling of the elastic modulus of thermal barrier coatings. *Surface and Coatings Technology*, 220, 170–173. doi:10.1016/j.surfcoat.2012.05.031

Sachit, T. S., Nandish, R. V., & Mallikarjun, . (2018). Thermal analysis of Cr_2O_3 coated diesel engine piston using FEA. *Materials Today: Proceedings*, 5(2), 5074–5081. doi:10.1016/j.matpr.2017.12.086

Śliwa, Miłkuta, Gołombek, Tański, Kwaśny, Bonek, & Brytan. (2016). Prediction of the properties of PVD/CVD coatings with the use of FEM analysis. *Applied Surface Science*, 388(A), 281-287. 10.1016/j.apsusc.2016.01.090

Pragyan Tiwari is a post graduate research student in the School of Mechanical Engineering at KIIT University. She has successfully completed her MTech in Mechanical System Design. Her area of research is piston simulation and design.